

Taming the ϵ_K in Little Randall Sundrum Models

Giancarlo D'Ambrosio^{1,2}, Mathew Thomas Arun², Ashwani Kushwaha^{2,1}, and Sudhir K. Vempati²

¹INFN-Sezione di Napoli, Complesso Universitario di Monte S. Angelo, Via Cintia Edificio 6, 80126 Napoli, Italy

² Centre for High Energy Physics, Indian Institute of Science, C. V. Raman Avenue, Bangalore 560012, India

May 25, 2022

Abstract

The neutral Kaon system puts strong constraints on many new physics models. The CP violating observable ϵ_K , in Randall Sundrum scenario, requires the lightest KK gluon to be heavier than ~ 24 TeV, whereas, in the Little Randall Sundrum models, the constraint is even stronger, $\gtrsim 32$ TeV. We show that stringent constraints can be relaxed in the presence of the Brane Localised Kinetic Terms (BLKT). In particular, for a range of values, a UV BLKT could significantly modify the lightest KK gluon wave function such that the limit reduces to 5 TeV. We also show that such a relaxation of the constraints can also be achieved by imposing flavour symmetries à la Minimal Flavour Protection.

1 Introduction

Flavour observables have been at the forefront of constraining physics beyond Standard Models. Precision observations of rare decays with high experimental accuracy have put significant constraints on new physics. The rare $\mu \rightarrow e + \gamma$ decay with a branching fraction limit of the $\sim \mathcal{O}(10^{-13})$ is one such example which puts severe constraints on various supersymmetric and extra-dimensional theories. In the hadronic sector the neutral K meson system puts the strongest constraint through observables such as Δm_K , ϵ_K and ϵ'/ϵ . Of all the three, ϵ_K remains the strongest constraint (For recent reviews, please see [1, 2, 3, 4, 5]). Randall Sundrum [6, 7] models too have been subjected to this scrutiny by the neutral K meson system [8, 9].

In the Randall Sundrum (RS) model the dominant new contribution to the $K^0 - \bar{K}^0$ mixing comes through the exchange of lowest KK gluon ($g^{(1)}$) at the tree level. To be compatible with the experiments, the lower limit on the mass of the $g^{(1)}$ should be of the $\mathcal{O}(24 \text{ TeV})$. This limit is very stringent and rules out any possibility of producing $g^{(1)}$ at the LHC.

The Little Randall Sundrum (Little RS) model [10, 11] is a version of the RS model where the UV scale is reduced to $\Lambda \sim 100 \text{ TeV}$ from the Planck scale. The attractive features of this model include enhanced signals at LHC, suppressed contributions to electro-weak precision observable [10] etc. However, the constraints from ϵ_K turn for the worse, they become more stringent [12]. A direct comparison between RS and Little RS would be misleading as the same bulk mass parameters would not fit fermion masses and mixing. A more accurate comparison would be to fit the fermion masses in both models and compare the likely lower bound on the mass of $g^{(1)}$. It is shown that the limit is $\sim \mathcal{O}(32 \text{ TeV})$, an increase of about 30%. Thus it would be interesting to see for mechanisms which could soften the constraints on Little RS.

Brane Localised Kinetic Terms (BLKTs) have been first discussed in the context of gravity [13] and for counterterms arising from loop correction to bulk field propagators [14] in extra dimensions with orbifold. Later, the idea was successfully applied to gauge theories [15, 16] to solve the “little” hierarchy problem coming from the electro-weak sector in the RS model. The flavour in Little RS has a similar pathology. Hence, it would be natural to ask whether BLKT could solve also the the flavour problem in the model. We show that for a range of values for the BLKTs, the lower limits on $g^{(1)}$ can be softened significantly.

Another interesting approach would be the application of flavour symmetries like U(2) or U(3). In the context of RS models, this has been used by [17], as Minimal Flavour Protection (MFP). We apply this paradigm to the Little RS model and show that the bounds on $g^{(1)}$ can become as low as 5 TeV.

The paper is organised as follows. In the next section we review the Little RS model, and along the way set up the notation used in the rest of the paper. In Sec.3 we will detail the computation of ϵ_K in the little RS model. In the next section, Sec.4, we discuss the Little RS model in the presence of Brane Localised Kinetic Terms and compute the constraints from ϵ_K . Sec.5 is devoted to imposition of flavour symmetries U(2) and U(3) and their implications. We end with a small summary and outlook.

2 Recap of the little RS model

To make the present paper self contained, we briefly recap the Little RS model in this section. The extra-dimensional set up is similar to Randall Sundrum model [6] with the background metric defined on

a $M_4 \times S^1/Z_2$ orbifold with a negative bulk cosmological constant. This geometry is defined by the line element

$$ds^2 = g^{MN} g_{MN} = e^{-2ky} \eta_{\mu\nu} dx^\mu dx^\nu + dy^2 \quad (1)$$

where $\eta_{\mu\nu} = \text{diag}(-1, +1, +1, +1)$ and $0 \leq y \leq L$. The warp factor, k is set such that $kL \sim 7$ with the fundamental scale $M_5 \sim \mathcal{O}(10^3 \text{ TeV})$ [10].

We assume the bulk to be populated by gauge fields and fermions transforming under the adjoint representation and fundamental representation of the Standard Model gauge group $SU(3) \times SU(2)_L \times U(1)_Y$ respectively [8]. The Higgs field, which transforms as a doublet under the weak gauge group, is assumed to be localised on the IR brane. This stabilises the Higgs vacuum expectation value to $\langle H \rangle = M_5 e^{-kL} \sim \mathcal{O}(1 \text{ TeV})$. The fermionic content includes three copies of the left handed quark doublets, $\hat{Q}^i, i = 1, 2, 3$, and three copies of right handed singlets, $\hat{q}^i = \hat{u}^i, \hat{d}^i$. Since the Clifford algebra in 5-dimension, given by five 4×4 Gamma matrices (Γ^M) , is non-reducible, the fermion representations in this geometry have 4 complex degrees of freedom. Hence, on breaking the 5-dimensional Lorentz group down to 4-dimensions via compactification these fermions become vector like under the Weyl representation of the 4-dimensional Clifford algebra. The orbifolding ensures that the unwanted set of chiralities are projected out from the lowest modes.

The five dimensional fermionic action for doublet(\hat{Q}) and singlet(\hat{q}) quarks with bulk mass terms is given as,

$$S_{\text{fermion}} = S_{\text{kin}} + S_{\text{Yuk}} \quad (2)$$

$$S_{\text{kin}} = \int d^5x \sqrt{-g} \left[\bar{\hat{Q}} (\Gamma^M D_M + m_Q) \hat{Q} + \sum_{q=u,d} \bar{\hat{q}} (\Gamma^M D_M + m_q) \hat{q} \right] \quad (2)$$

$$S_{\text{Yuk}} = \int d^5x \sqrt{-g} \left(\left(\tilde{Y}_u^{(5)} \right)_{ij} \bar{\hat{Q}}_i \hat{u}_j + \left(\tilde{Y}_d^{(5)} \right)_{ij} \bar{\hat{Q}}_i \hat{d}_j \right) H(x^\mu) \delta(y - L) + h.c., \quad (3)$$

where m_Q and m_q are the bulk masses for the doublet and singlet quark field respectively, i, j are generational indices and $\left(\tilde{Y}_{u,d}^{(5)} \right)_{ij}$ are the five dimensional Yukawa coupling matrices. In the above equation, D_M represent the covariant derivative in 5-dimensions. The following boundary conditions, at the orbifold fixed points ($y = 0, y = L$), ensure correct chiral projections for the lowest modes;

$$\hat{Q}_l(++), \hat{Q}_r(--), \hat{q}_l(--), \hat{q}_r(++), \quad (4)$$

where l, r stand for left and right chiral fields under the 4-dimensional chiral projection operator and $+(-)$ stands for the Neumann (Dirichlet) boundary conditions.

The Kaluza-Klein decomposition of a generic fermion field (Q) is given by

$$Q(x, y)_{l,r} = \sum_{n=0}^{\infty} \frac{1}{\sqrt{L}} Q_{l,r}^{(n)}(x) f_{l,r}^{(n)}(y, c), \quad (5)$$

where $Q_{l,r}^{(n)}(x)$ stands for the corresponding four dimensional chiral KK modes and $f_{l,r}(y)$ are profiles of these modes in the bulk set to satisfy the ortho-normality condition

$$\int_0^L dy e^{-3ky} f_{l,r}^{(n)} f_{l,r}^{(m)} = \delta_{n,m}. \quad (6)$$

For the zero mode the profile takes the form

$$f_l^{(0)}(y, c_{Q_i}) = \sqrt{k} f^0(c_{Q_i}) e^{ky(2-c_{Q_i})} e^{(c_{Q_i}-0.5)kL} \quad (7)$$

$$f_r^{(0)}(y, c_{q_i}) = \sqrt{k} f^0(c_{q_i}) e^{ky(2-c_{q_i})} e^{(c_{q_i}-0.5)kL} \quad (8)$$

where,

$$f^0(c) = \sqrt{\frac{(1-2c)}{1-e^{-(1-2c)kL}}} \quad (9)$$

and the bulk mass parameters are defined as $c_Q = m_Q/k$ for doublet quarks and $c_q = -m_q/k$ for singlet. In this paper we are not interested in the higher KK modes of fermions and their contribution will always be suppressed by $\sim \mathcal{O}(\langle H \rangle / M_{KK})$, where M_{KK} is the compactification scale. Inserting the zero mode profile into the Yukawa action given in Eq.2, we obtain the effective 4D Yukawa coupling relevant for the SM fermion masses and mixings as,

$$\begin{aligned} Y_{d_{ij}} &= f^0(c_{Q_i}) \left(Y_d^{(5)} \right)_{ij} f^0(c_{d_j}) \\ Y_{u_{ij}} &= f^0(c_{Q_i}) \left(Y_u^{(5)} \right)_{ij} f^0(c_{u_j}) \end{aligned} \quad (10)$$

where $\mathcal{O}(1)$ Yukawa ($Y_{u,d}^{(5)}$) parameters entering the mass matrices are defined as:

$$Y_{u,d}^{(5)} \equiv k \tilde{Y}_{u,d}^{(5)} \quad (11)$$

The transformation from the quark flavour eigenbasis $\hat{u}_{l,r}, \hat{d}_{l,r}$ to the mass eigenbasis $u_{l,r}, d_{l,r}$ will then be given by performing rotation of unitary mixing matrices $U_{l,r}$ and $D_{l,r}$ as

$$u_{l,r} = U_{l,r}^\dagger \hat{u}_{l,r}, \quad d_{l,r} = D_{l,r}^\dagger \hat{d}_{l,r}. \quad (12)$$

With this the CKM matrix is given by

$$V_{CKM} = U_l^\dagger D_l \quad (13)$$

It should be noted that there is no reason for bulk fermionic masses to be diagonal or real. Since we are not assuming Minimal Flavour Violation(MFV), the Unitary matrices that diagonalise these bulk mass terms do not diagonalise the five dimensional Yukawa Lagrangian.

Gauge couplings To derive the bulk wave profile and coupling of the gauge boson with fermion bilinear it suffices to describe a $U(1)$ gauge group in the bulk of the AdS. The generalisation to non-abelian gauge fields is straight forward. The five dimensional action for such a gauge field is given as

$$\mathcal{S} = -\frac{1}{4g_5^2} \int d^5x \sqrt{-g} (g^{CM} g^{DN} F_{CD} F_{MN}) \quad (14)$$

where the field strength tensor $F_{MN} = \partial_M A_N - \partial_N A_M$ and g_5^{-2} is the 5D gauge coupling.

In the unitary gauge, the vector field can be Fourier expanded as

$$A_\mu(x, y) = \sum_n f_A^{(n)}(y) A_\mu^{(n)}(x), \quad (15)$$

where $A_\mu^{(n)}(x)$ are the 4D gauge field KK modes and $f_A^{(n)}(y)$ are profiles of these modes in the bulk. The equations of motion are given as by

$$-\partial_5 \left(e^{-2ky} \partial_5 f_A^{(n)} \right) = m_n^2 f_A^{(n)}. \quad (16)$$

On integrating the above equation and demanding the zero KK mode be non vanishing, we arrive at the boundary condition $(\delta A^\mu \partial_y A_\mu)|_{0,L} = 0$. For canonical kinetic terms, the orthonormality condition is

$$\int_0^L dy f_A^{(n)} f_A^{(m)} = \delta_{nm}. \quad (17)$$

For the gauge zero modes the profile is flat in the extra dimension and is given as

$$f_A^{(0)}(y) = \frac{1}{\sqrt{L}} \quad (18)$$

For the higher KK modes ($m_n \neq 0$) the solution is given in terms of the Bessel J and Y functions and is of the form:

$$f_A^{(n)}(y) = N_A^{(n)} e^{ky} \left[J_1 \left(\frac{m_n}{k e^{-ky}} \right) + b_A^{(n)} Y_1 \left(\frac{m_n}{k e^{-ky}} \right) \right] \quad (19)$$

$N_A^{(n)}$ are the the normalisation constants. The coefficients b_A^n are determined at the boundaries as

$$b_{UV}^{(n)} = -\frac{J_0(\frac{m_n}{k})}{Y_0(\frac{m_n}{k})}, \quad b_{IR}^{(n)} = -\frac{J_0(\frac{m_n}{k} e^{kL})}{Y_0(\frac{m_n}{k} e^{kL})}. \quad (20)$$

Equating $b_{UV}^{(n)} = b_{IR}^{(n)}$ we get the spectrum $m_n = x_n k e^{-kL}$ where x_n are the roots of this equation.

The coupling of the zero mode fermions with the gauge KK modes is set by the overlap integral [18]

$$g_{l,r}^{(n)}(c_{Q,q}) = g_5 \int_0^L dy e^{-3ky} f_A^{(n)}(y) f_{l,r}^{(0)}(y, c_{Q,q}) f_{l,r}^{(0)}(y, c_{Q,q}) \quad (21)$$

where $f_{l,r}^{(0)}$ and $f_A^{(n)}$ are given by Eq.9 and Eq.19 respectively. Note that this function is quite sensitive to the UV scale and changing the scale could significantly modify the low energy phenomenology. Figure 1 shows the difference between the coupling of KK-1 gluon in RS and Little RS and it could be seen that the coupling is enhanced by a factor 3 in the Little RS in comparison to RS for the fermion with the same 'c' value. This could be understood from the fact that, since the fundamental scale is much smaller, the UV localised fermions have bigger overlap with the composite gauge boson states.¹ This has important implications for LHC phenomenology and ϵ_K as will be demonstrated shortly.

A further important point regarding the coupling in Eq.21 is that it is non-universal in generational space. This is evident when we explicitly write these couplings down as:

$$g_l^{(n)}(c_{Qi}) \bar{\hat{Q}}_l^{i(0)} \gamma_\mu G^{\mu(n)} \hat{Q}_l^{i(0)} + g_r^{(n)}(c_{ui}) \bar{\hat{u}}_r^{i(0)} \gamma_\mu G^{\mu(n)} \hat{u}_r^{i(0)} + g_r^{(n)}(c_{di}) \bar{\hat{d}}_r^{i(0)} \gamma_\mu G^{\mu(n)} \hat{d}_r^{i(0)} \quad (22)$$

After electroweak symmetry breaking, unitary transformations ($D_{l,r}$, $U_{l,r}$) of Eq.12 are used to go to mass eigen basis. This non-universality in couplings leads to flavour violation in these models.

¹For the IR localised fermions, one would expect the situation to be opposite, a reduction in the coupling.

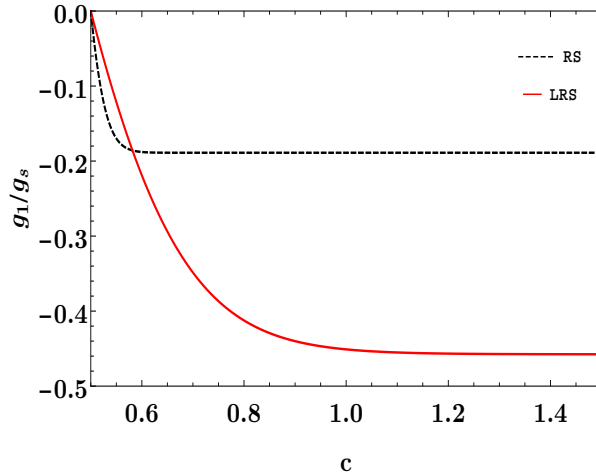


Figure 1: A comparison of coupling of first KK gluon with light fermions as a function of the c values in RS (blue/dotted) and Little RS (red/solid)

Phenomenological constraints The RS model addresses Higgs mass hierarchy problem; however, the wave function modification of the SM Z_μ and W_μ gauge bosons at the IR brane, due to the localization of the Higgs, brings about large tree level contributions to the electro-weak observables [8, 19, 16]. This correction to the Peskin-Takeuchi parameters [20], S and T, was shown [19] to be $\propto -(kL)\frac{v^2}{M_{KK}^2}$. The S-parameter, though, could be lowered significantly [8, 16, 21, 22] owing to the fact that the elementary sector is localised at the UV brane and their couplings remain unchanged due to the IR brane modifications. On the other hand, the T-parameter remains large and for a 125 GeV Higgs, in RS with $kL \sim 33$, the lower limit on mass of the KK excitation set to satisfy the LEP bound at 1σ turns out to be ~ 13.6 TeV [22]. Thus loosing the predictability of the model at the current LHC and this brings in “little hierarchy” for the Higgs mass. The T-parameter enhancement could be solved either by adjusting operators in the IR brane, such that the contribution could be canceled, or by truncating the volume of the extra dimension.

Assuming the $kL \sim 7$ the truncated space brings down the tree level contribution to the T-parameter. The left-over correction due to KK partner contribution to the loop could be summarised by the dimension six operator $\frac{1}{\Lambda^2}(D^\mu H)^\dagger H(H^\dagger D_\mu H)$ and it amounts to a compactification scale $M_{KK} \sim 4$ TeV [10].

Another important expectation from the Little RS model is the ‘enhancement’ of the collider signal compared to the RS. Since at LHC the production of the lightest KK gluon and Z boson at s-channel proceeds via the annihilation of the UV localised quarks, from Figure 1 we can estimate that the production cross-section for the process must be larger for the Little RS. The recent search for heavy particles that decay into top-quark pair from ATLAS [23] performed using the data collected from 13 TeV LHC, with an integrated luminosity of $36.1 fb^{-1}$, rules out the masses smaller than ~ 3.6 TeV at 95% CL for the KK gluon with a branching fraction of 30%. The strong coupling of light fermions to these gluon excitations were set to $-0.2g_s$, where g_s is the strong coupling of the SM gluon. The left handed coupling of the top quark was taken to be g_s and the right handed coupling was fixed by demanding the required branching fraction. The analysis considered the process $pp \rightarrow t\bar{t}$ with top decaying in to $t \rightarrow bW$ with events selected requiring single charged isolated lepton, jets, missing transverse energy (or \cancel{p}_T). SM background processes

were reduced by requiring the jets identified as likely to contain b-hadrons. We use this ATLAS data to constrain our model.

While these limits hold for the RS model, we would use the couplings and branching fractions demanded by the bulk mass parameters of our model given in Table 2. These parameters were chosen such that it would satisfy the CKM matrix and will be useful for our further analysis of ϵ_K . Hence, a direct comparison to the limit give by ATLAS for the RS model is not the intention of this section, rather our aim is to find the lightest mass of KK gluon in our model allowed by LHC.

We have used CalcHEP 3.7.5 [24] with NNPDF2.3 with QED corrections to compute the cross section of the process $q q \rightarrow g^{(1)} \rightarrow t \bar{t}$ in Little RS model with $e^{-kL} = 10^{-3}$ and the bulk mass parameters of the fermions given in Table 2. Since we have not mentioned a specific K-factor CalcHEP uses a version of this function which always returns 1. With these considerations we have found that the mass of the first KK partner of the gluon should be greater than ~ 4.2 TeV as shown in Figure 2.

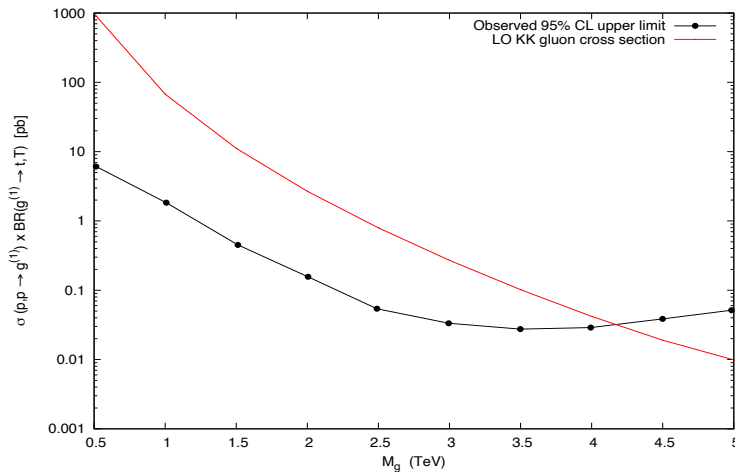


Figure 2: The observed cross-section 95% CL upper limit [23] on the g_1 signal and the theoretical prediction for the production cross-section times branching ratio of $g_1 \rightarrow t \bar{t}$ at corresponding masses

3 ϵ_K in Little RS

Other than the hadron collider and LEP limits mentioned in the previous section, the neutral meson mixing, especially the CP-Violation observable (ϵ_K) from $K^0 - \bar{K}^0$, have been shown to constraint the scale of RS [17, 25, 26, 27, 28, 29] and Little RS [26, 12] models significantly. In particular, it is more worrying for the Little RS scenario since, as shown in Figure 1, the light fermions couple stronger to KK gauge boson states

than in RS. And in such case, it is imperative that we should analyse the mixing in this model and tame it before making any predictions. Here, in this section, we aim to recall the important results of $\Delta F = 2$ process in warped geometry.

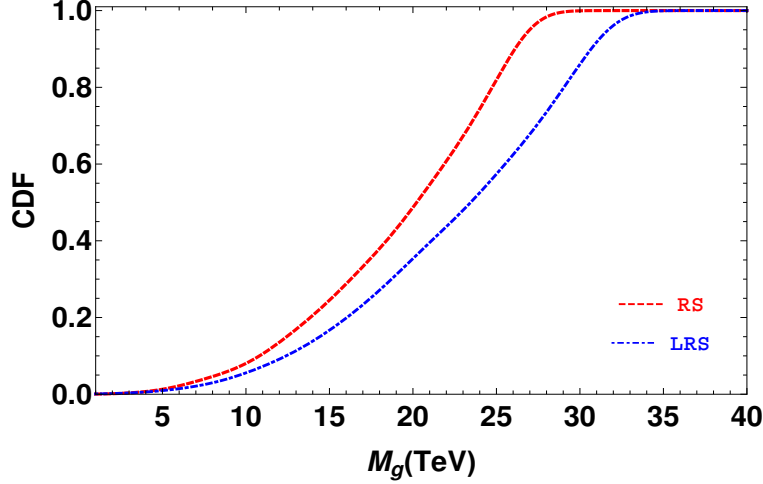


Figure 3: CDF for M_g from ϵ_K (analysis performed from the dominant $|Im C_4^{sd}|$) for RS and LRS model. Dashed lines correspond to the RS and dash-dot to LRS.

Note that from Eq.21 the coupling of the bulk gauge boson KK states to fermion bilinear are dependent on the bulk mass parameter of the fermion. This renders the couplings family non-universal in the gauge basis. On rotating to the mass basis, defined by $D_{l,r}$ and $U_{l,r}$ given in the Appendix, the couplings become flavour non-diagonal. In principle all the gauge KK states would contribute to this process, but the dominant contribution comes from the tree level exchange of the lightest gluon KK state. On integrating out the new physics with mass M_g , the effective Hamiltonian for $\Delta F = 2$ becomes [28],

$$H_{eff} = \frac{1}{M_g^2} \left[g_l^{ij} g_l^{km} (\bar{d}_l^{i\alpha} T_{\alpha\beta}^a \gamma_\mu d_l^{j\beta}) (\bar{d}_l^{k\delta} T_{\delta\rho}^a \gamma_\mu d_l^{m\rho}) + g_r^{ij} g_r^{km} (\bar{d}_r^{i\alpha} T_{\alpha\beta}^a \gamma_\mu d_r^{j\beta}) (\bar{d}_r^{k\delta} T_{\delta\rho}^a \gamma_\mu d_r^{m\rho}) + (l \leftrightarrow r) \right], \quad (23)$$

where T^a are the QCD generators, latin indices i, j, k, l, m and the greek indices denote fermion generations and colour respectively. Couplings $g_{l,r}$ are defined as;

$$g_l = D_l^\dagger g_l^{(1)}(c_Q) D_l, \quad g_r = D_r^\dagger g_r^{(1)}(c_d) D_r, \quad (24)$$

where $g_l^{(1)}(c_Q)$ and $g_r^{(1)}(c_d)$ are the gluon couplings defined in Eq.21. Using the unitarity of $D_{l,r}$, the above expression could be further expanded to understand the $\Delta F = 2$ transitions in first and second generations. For this process, we only require the off diagonal elements which represent the flavour violating couplings and are given as,

$$\begin{aligned} g_l^{12} &= D_l^{(21)*} D_l^{(22)} \left(g_l^{(1)}(c_{Q2}) - g_l^{(1)}(c_{Q1}) \right) + D_l^{(31)*} D_l^{(32)} \left(g_l^{(1)}(c_{Q3}) - g_l^{(1)}(c_{Q1}) \right) \\ g_r^{12} &= D_r^{(21)*} D_r^{(22)} \left(g_r^{(1)}(c_{d2}) - g_r^{(1)}(c_{d1}) \right) + D_r^{(31)*} D_r^{(32)} \left(g_r^{(1)}(c_{d3}) - g_r^{(1)}(c_{d1}) \right) \end{aligned} \quad (25)$$

Using the Fierz identity and quadratic Casimir, the above expression could be simplified to

$$H_{eff} = \frac{1}{M_g^2} \left[g_l^{ij} g_l^{km} \frac{1}{2} \left((\bar{d}_l^{i\alpha} \gamma_\mu d_l^{j\delta}) (\bar{d}_l^{k\delta} \gamma_\mu d_l^{m\alpha}) - \frac{1}{N_C} (\bar{d}_l^{i\alpha} \gamma_\mu d_l^{j\alpha}) (\bar{d}_l^{k\delta} \gamma_\mu d_l^{m\delta}) \right) \right. \\ \left. - g_r^{ij} g_l^{km} ((\bar{d}_r^{i\alpha} d_l^{m\alpha}) (\bar{d}_l^{k\delta} d_r^{j\delta}) + \frac{1}{N_C} ((\bar{d}_r^{i\alpha} d_l^{m\delta}) (\bar{d}_l^{k\delta} d_r^{j\alpha})) + (l \leftrightarrow r) \right] \quad (26)$$

Adopting the usual parametrization of new physics effects in Kaon oscillation [30, 31] we can write the model independent Effective Hamiltonian as

$$H^{\Delta S=2} = \sum_{a=1}^5 C_a \mathcal{O}_a^{sd} + \sum_{a=1}^3 \tilde{C}_a \tilde{\mathcal{O}}_a^{sd}. \quad (27)$$

In the above equation, the first set of operators C_a contain left handed chiral states and the operators \tilde{C}_a contain right chiral set of states. And the relevant operators \mathcal{O} are,

$$\begin{aligned} \mathcal{O}_1^{sd} &= (\bar{d}_l^\alpha \gamma_\mu s_l^\alpha) (\bar{d}_l^\beta \gamma_\mu s_l^\beta), \\ \mathcal{O}_4^{sd} &= (\bar{d}_r^\alpha s_l^\alpha) (\bar{d}_l^\beta s_r^\beta), \quad \mathcal{O}_5^{sd} = (\bar{d}_r^\alpha s_l^\beta) (\bar{d}_l^\beta s_r^\alpha), \end{aligned} \quad (28)$$

and $\tilde{\mathcal{O}}_i$ is given by exchanging $l \leftrightarrow r$ in \mathcal{O}_i . Comparing the above expressions for the operators with the Effective Hamiltonian given in Eq.(26), we could infer

$$C_1 = \frac{1}{M_g^2} g_l^{12} g_l^{12} \left[\frac{1}{2} \left(1 - \frac{1}{N_C} \right) \right], \quad C_4 = \frac{1}{M_g^2} g_l^{12} g_r^{12} [-1], \quad C_5 = \frac{1}{M_g^2} g_l^{12} g_r^{12} \left[\frac{1}{N_C} \right]. \quad (29)$$

Since the CP-Violating ϵ_K parameter in terms of the Effective Hamiltonian Eq.27 is given as,

$$\epsilon_K \propto \text{Im} \langle K^0 | H^{\Delta S=2} | \bar{K}^0 \rangle, \quad (30)$$

only the imaginary parts of the Wilson coefficients contribute and the bound on M_g from Eq.29 can be summarised as

Im(Wilson coeff.)	Bound (TeV)
Im(C_1)	1.5×10^3
Im(C_4)	1.6×10^4
Im(C_5)	1.4×10^4

Table 1: Lower limit on Wilson coefficients at scale 3 TeV [25]. The Wilson coefficients are given at the scale Λ [32], which are adapted here for the renormalisation group scaling from Λ to 3 TeV.

The model independent bound from ϵ_K is strongest on the Wilson coefficient C_4 due to (as compared to C_1) chiral enhancement of the hadronic matrix element and the RG running from the new physics scale to the hadronic scale [30, 33, 34].

With the above formalism in place, comparison of the constraint coming from ϵ_K in RS and Little RS model would be rendered simple since the difference between these models arise through the off diagonal couplings $g_{l,r}^{12}$ in the respective scenarios. For numerical study, we fit the bulk quark mass parameters to obtain the spectrum in $\bar{M}S$ scheme computed at 3 TeV while keeping the 5D Yukawa anarchic ($0.1 \leq |Y_{u,d_{ij}}^{(5)}| \leq 3$). We refrain from discussing the procedure here, but the detailed methodology for the numerical analysis can be found in Appendix A.

In Figure 3, we present our result showing the dependence of the cumulative distribution functions (CDF) for the number of states satisfying the ϵ_K observable ($|ImC_4^{sd}|$) with varying KK gluon mass scale M_g for both RS and Little RS. It can easily be read that the average value of ϵ_K becomes consistent with the measurement for only $M_g \geq 24$ TeV for RS and $M_g \geq 32$ TeV for Little RS.

One of the naive understanding from Eq.21 and Eq.29 could be infer that, if the value of g_5 could be reduced, the bounds on the operators $C_{1,4,5}$ could be reduced. This could be achieved by the RG running of the gauge coupling as well as with Brane Localised Kinetic Terms. This possibility have been mentioned in the [25, 27] within the context of RS models.

4 Brane Localised Gauge Kinetic Terms

To that end, lets start by deriving the wavefunction and the KK mass eigenvalue equation for the bulk gauge fields with Brane Localised Kinetic Terms (BLKT) in the Little RS scenario. Here, we further compute the couplings of the gauge field KK mode to KK-0 mode of the fermions and demonstrate, how presence of BLKT could change them. As a toy model, lets start by performing a calculation for a $U(1)$ gauge field. This could easily be generalised to the case of non-Abelian fields, since we are only interested in the gauge interaction with the fermion bilinear. The generalisation to the gauge 5-dimensional action given in Eq.14, including the BLKT, could be written as[15, 16]

$$\mathcal{S} = -\frac{1}{4g_5^2} \int d^5x \sqrt{-g} \left(g^{AM} g^{BN} F_{AB} F_{MN} + [l_{IR}\delta(y-L) + l_{UV}\delta(y)] g^{\alpha\mu} g^{\beta\nu} F_{\alpha\beta} F_{\mu\nu} \right) \quad (31)$$

Here, we have chosen the convention where the mass dimension of the 5-dimensional gauge field remains $[A_\mu(x, y)] = 1$ and hence g_5^{-2} becomes dimensional.

Unlike Eq.16 in the previous section, in the presence of BLKT, the new equation of motion derived from Eq.31 becomes,

$$-\partial_5(e^{-2ky}\partial_5 f_A^{(n)}) = (1 + l_{IR}\delta(y-L) + l_{UV}\delta(y))m_n^2 f_A^{(n)}. \quad (32)$$

and the new ortho-normality condition becomes,

$$\int_0^L dy [1 + l_{IR}\delta(y) + l_{UV}\delta(y-L)] f_A^{(n)} f_A^{(m)} = \delta_{nm}, \quad (33)$$

The solution to the equation could be derived as,

$$f_A^{(n)}(y) = N_A^{(n)} e^{ky} \left[J_1 \left(\frac{m_n}{ke^{-ky}} \right) + b_A^{(n)} Y_1 \left(\frac{m_n}{ke^{-ky}} \right) \right] \quad (34)$$

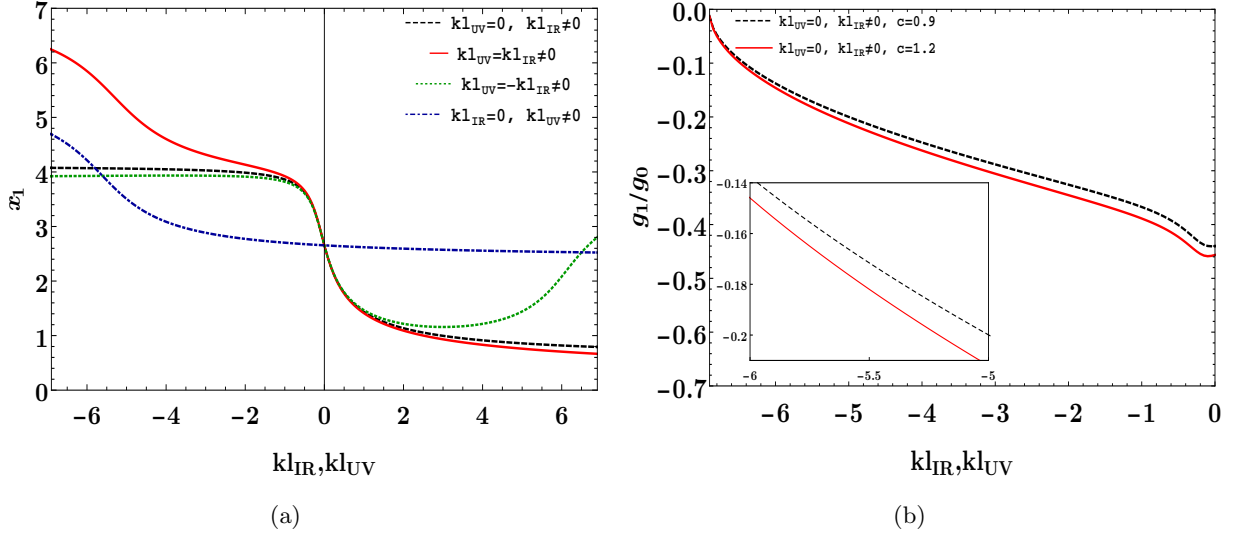


Figure 4: (a) The behaviour of the first root as function of l_{IR} and l_{UV} . Four different situation has been considered: (i) $kl_{UV} = 0$ (black dashed), (ii) $kl_{IR} = 0$ (Blue Dot-dashed), (iii) $kl_{IR} = l_{UV}$ (red solid) and (iv) $kl_{IR} = -kl_{UV}$ (green dotted) (b) The ratios of the first KK mode to that of the zero-mode of Gauge couplings with fermions as a function of kl_{UV} and kl_{IR} . The couplings for $kl_{UV} = 0, kl_{IR} \neq 0, c = 0.9$ (Black Dashed), $c = 1.2$ (Red) are labelled.

where $(N_A^{(n)})$ is the normalisation constant and the new zero mode wavefunction becomes,

$$f_A^{(0)}(y) = \frac{1}{\sqrt{L + l_{IR} + l_{UV}}} . \quad (35)$$

Integrating the equation of motion around the fixed points $y = 0$ and $y = L$ yields the modified boundary conditions,

$$\begin{aligned} \partial_y f_A^{(n)}|_0 &= -l_{UV} m_n^2 f_A^{(n)}(0) , \\ \partial_y f_A^{(n)}|_L &= +e^{2kL} l_{IR} m_n^2 f_A^{(n)}(L) \end{aligned} \quad (36)$$

Demanding that the solution Eq.34 should satisfy the boundary condition, the $b_A^{(n)}$ becomes,

$$b_A^{(n)}|_{UV} = -\frac{J_0(\frac{m_n}{k}) + m_n l_{UV} J_1(\frac{m_n}{k})}{Y_0(\frac{m_n}{k}) + m_n l_{UV} Y_1(\frac{m_n}{k})} , \quad (37)$$

$$b_A^{(n)}|_{IR} = -\frac{J_0(\frac{m_n}{k} e^{kL}) - m_n l_{IR} e^{kL} J_1(\frac{m_n}{k} e^{kL})}{Y_0(\frac{m_n}{k} e^{kL}) - m_n l_{IR} e^{kL} Y_1(\frac{m_n}{k} e^{kL})} , \quad (38)$$

where $m_n = x_n k e^{-kL}$, and x_n are the roots of the master equation obtained by imposing $b_A^{(n)}|_{UV} = b_A^{(n)}|_{IR}$. The dependence of the first root, x_1 , on BLKT is shown in the Figure 4(a) for the geometry defined by $k = 10^3$ TeV. As can be seen $x_1 \sim 2.7$ when the BLKTs are zero. Four interesting cases of non-zero BLKTs (i) $kl_{UV} = 0, kl_{UV} \neq 0$, (ii) $kl_{UV} = kl_{UV} \neq 0$, (iii) $kl_{UV} = -kl_{UV} \neq 0$ and (iv) $kl_{UV} \neq 0, kl_{UV} = 0$. As can be seen the lowest root itself can modify by roughly a factor between 2 and 3 for the case (ii), when both the BLKTs are switched on.

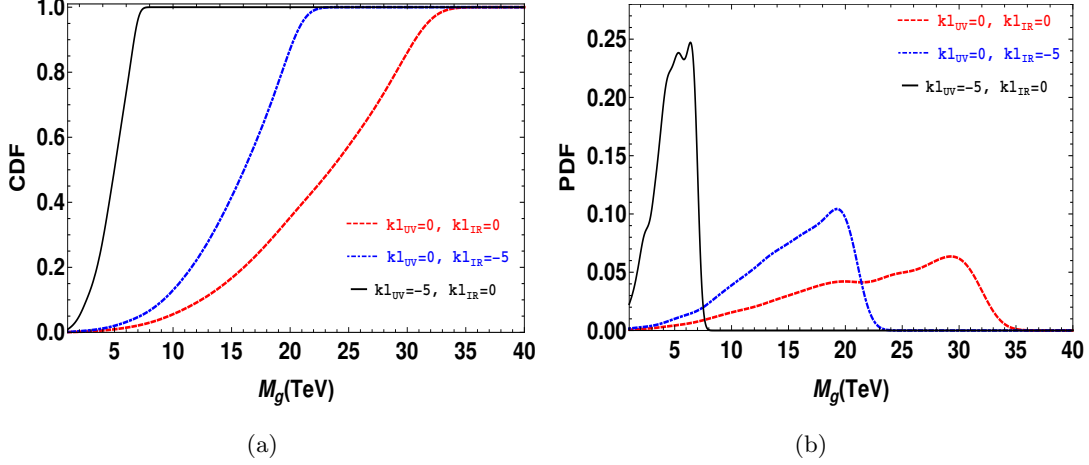


Figure 5: PDF and CDF of $Im(C_4)$ in three different scenarios: (a) $l_{UV} = l_{IR} = 0$ (red dash) (b) $kl_{UV} = 0, kl_{IR} = -5.0$ (blue dot-dash)(c) $kl_{UV} = -5, kl_{IR} = 0$.(black solid)

Now, along with the modification of the roots, BLKT modifies the bulk gauge field wave profile as shown in Eq.34 and hence the overlap of the gauge boson with the fermion wave profile. With that the modified gauge coupling becomes,

$$\begin{aligned}
g_{l,r}^{(n)}(c_{Q,q}) &= g_5 \int_0^L dy e^{-3ky} f_A^{(n)}(y) f_{l,r}^{(0)}(y, c_{Q,q}) f_{l,r}^{(0)}(y, c_{Q,q}) \\
&= g_4 \sqrt{L + l_{IR} + l_{UV}} \int_0^L dy e^{-3ky} f_A^{(n)}(y) f_{l,r}^{(0)}(y, c_{Q,q}) f_{l,r}^{(0)}(y, c_{Q,q}) ,
\end{aligned} \tag{39}$$

where we have used the zero mode gauge coupling g_4 to redefine g_5 .

This modification could have significant impact on flavour physics. Again, going through the same analysis as the one performed for the vanishing BLKT scenario in Sec.3 and using the constraint on C_4 operator given there, we see that the BLKT strength has a notable effect on the ϵ_K parameter. This could be understood better from Figure 4, where we have displayed the $g^{(1)}$ coupling with the first two generation quark bilinear (with bulk mass parameter $c = 0.9$ and $c = 1.2$ chosen for better contrast and clarity). Note that the couplings become comparable for large negative BLKT and as a result the couplings, $g_{l,r}^{12}$ in Eq.25 reduces.

The Cumulative Distribution Function (CDF) and the Probability Distribution Function (PDF) with respect to $M_{g(1)}$ are presented in Figure 5. The presence of reasonably large negative BLKT $kl \sim -5$ either the UV or at the IR reduces the constraint significantly. It is the UV localised BLKT, however which is more effective comparatively which reduces the limit from 35 TeV to around 5 TeV. Given the steep form of the distribution, it is clear that a part of this parameter space is probably visible at LHC. The result of this section is summarised in Table 3. It is clear that the BLKTs achieve this by bringing the couplings of the two light flavours closer to each other and thus it is only natural that this could be achieved by a flavour symmetry which we will explore in the next section.

A benchmark for the 'c' values used to do this calculation is given in Table 2.

Parameter	c_{Q1}	c_{Q2}	c_{Q3}	c_{d1}	c_{d2}	c_{d3}	c_{u1}	c_{u2}	c_{u3}
c	1.21	1.13	0.36	1.29	1.15	1.02	1.65	0.59	-0.80

Table 2: Sample point with the corresponding fits of observable tabulated in Table 3 for three scenarios without BLKT and with BLKT.

$kl_{IR} = kl_{UV} = 0$	$kl_{IR} = 0, kl_{UV} = -5$	$kl_{UV} = 0, kl_{IR} = -5$
30 TeV	8 TeV	20 TeV

Table 3: Lower bound on ImC_4 for three scenarios without BLKT and with BLKT for c values tabulated in Table 2.

5 Minimal Flavour Protection

Minimal Flavour Protection (MFP) [17] was introduced to suppress the chiral enhanced contributions to the $\Delta F = 2$ Hamiltonian. These are typically contained in C_4 and C_5 Wilson coefficients, while the Standard Model contributions are contained in C_1 . The MFP paradigm assumes a conserved chiral symmetry for the right handed down sector with a consequence of significantly suppressing the contributions from C_4 and C_5 . Its application to RS model is already discussed in literature.

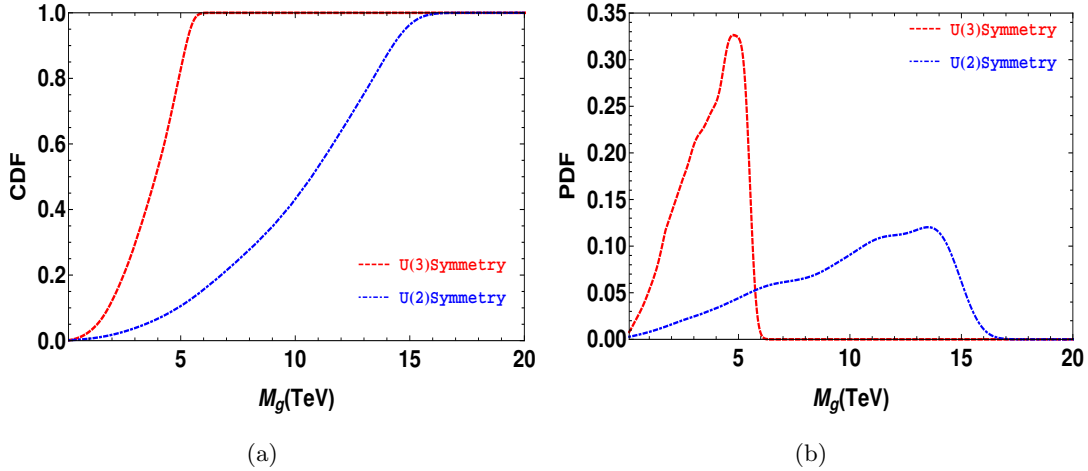


Figure 6: PDF and CDF of $Im(C_1)$ bounds for MFP in LRS (a) Unbroken $U(3)$ flavour symmetry (red dashed) and (b) $Im(C_4)$ bounds for $U(2)$ symmetry (blue dot-dash).

Similarly, in Little RS, the most important contribution comes from the C_4 coefficient. From Figure 3 the behaviour of C_4 coefficient in Little RS is worse than in RS and the new limit of the first KK excited gluon becomes $M_g \gtrsim 35$ TeV. Imposing the horizontal $U(3)$ symmetry, like before, prohibits such operators at first order. The leading bounds are now on the C_1 -coefficient. Higher order operators are generated at dimension-8 arise due to Higgs insertion, and then can be neglected. In this case we observe that for MFP,

bounds from C_1 operator is stronger than the C_4 .

Here we consider two different scenarios, one with exact $U(3)$ horizontal symmetry and the one where this symmetry gets broken down to a $U(2)$ involving the first two generations. When $U(3)$ flavour symmetry is assumed to be exact the bulk mass parameters for the right handed down sector becomes $c_{d1} = c_{d2} = c_{d3}$. We can observe from Eq.40, the non diagonal coupling for right handed component of $g_r^{12} = 0$, hence only C_1 operator is observable and as we observe in Figure 6 the bounds for LRS-MFP gets lowered to $M_g \sim 4$ TeV. On the other hand, in the case where the full symmetry is broken down to $U(2)$, the bounds on KK-1 gluon mass becomes $M_g \gtrsim 18$ TeV. In this consideration, the non-diagonal coupling corresponding to flavour violation in s and d quark is given as:

$$g_r^{12} = D_r^{(31)*} D_r^{(32)} \left(g_r^{(1)}(c_{d3}) - g_r^{(1)}(c_{d1}) \right) \quad (40)$$

Using the naive expression of D_r from Appendix[A] $\left(|D_r|_{ij} \sim \frac{f^{(0)}(c_{di})}{f^{(0)}(c_{dj})} \right)$, the g_r^{12} is given as

$$g_r^{12} \sim \frac{f^{(0)}(c_{d1})}{f^{(0)}(c_{d3})} \frac{f^{(0)}(c_{d2})}{f^{(0)}(c_{d3})} \left(g_r^{(1)}(c_{d3}) - g_r^{(1)}(c_{d1}) \right) \quad (41)$$

where $f^{(0)}(c_{di})$ dictates the masses of quark in down sector as shown in Eq.(10). For hierarchical masses $f^{(0)}(c_{d3}) > f^{(0)}(c_{d2}) > f^{(0)}(c_{d1})$, however with $U(2)$ imposed $f^{(0)}(c_{d2}) = f^{(0)}(c_{d1})$. Hence, the above expression states that if the mass difference in first-third generation and second-third generation is large, this could lead to decoupling and effect on flavour violation would be negligible. This feature is not restricted to Little RS but applies to most New Physics models [35, 36].

6 Summary and Outlook

Randall Sundrum models offer one of the elegant solutions not only to the hierarchy problem but also to the fermion mass hierarchies and mixing in terms of a geometric Froggatt-Nielsen mechanism. However the constraints from LEP are very stringent on these models restricting its ‘visibility’ at the LHC. The Little RS offers hope in that direction due to its lowered UV scale and thus larger couplings and overlap functions compared to the RS. But for the same reason, it also suffers stronger constraints from flavour physics compared to the RS. In this work we looked at the Kaon sector which has been emphasised in [12] and tried to propose two solutions that help in alleviating the concerns. The first one is the use of Brane Localised Kinetic Terms for the gluon wavefunction. The second one is to use of Minimal Flavour Protection flavour symmetries to restrict certain dominant operators. For large enough BLKTs we have seen that the constraints [17] reduce significantly. In the case of MFP the imposition of $U(3)$ works better compared to $U(2)$. While both these mechanisms work very differently, they are both efficient in reducing the constraints.

Phenomenologically we expect both these mechanisms to have significantly different implications especially for electroweak precision observables and LHC signatures. Before we close two comments are in order: (a) It would be definitely interesting to see the implications of the BLKTs and flavour symmetries on systems other than $s - d$ like $b - d$ or $b - s$. In some cases, BLKTs on the gluon field might not be

sufficient. (b) There could be other mechanisms like Minimal Flavour Violation (MFV) [37] which could as well suppress the New Physics contributions in a similar manner as MFP [38]. This would be interesting to explore as well.

Another line of research testing the $b-s$ -transitions is the B-anomalies [39]. Several models, leptoquarks, Z' , .., with New Physics scale of few TeV have been constructed in order to explain the so called B-anomalies [40, 41, 42, 43, 44, 45]. If B-anomalies are confirmed, due to the low scale of New Physics required, this will be kind of a revolution compared to the traditional paradigm of Minimal Flavour Violation where a gap is expected between the scale of the solution of the Naturalness problem and the MFV scale [39]. Our scenarios depart from MFV and seem suitable to address B-anomalies: we plan to pursue the set-ups studied here by looking for flavour signatures.

Acknowledgements

A.K. is supported by the INFN research initiative Exploring New Physics (ENP). M.T.A. acknowledges the support from UGC-DSKPDF. G.D. was supported in part by MIUR under Project No. 2015P5SBHT and by the INFN research initiative ENP. G.D. thanks “Satish Dhawan Visiting Chair Professorship” at the Indian Institute of Science. We thank IoE funds of IISc for support. SKV is supported by the project “Nature of New Physics” by the Department of Science and Technology, Govt. of India.

A Flavour Parameters and Numerical Analysis

In this section we analyze the independent flavour parameters in the quark sector and discuss the full parameter scan of c values of quark, which could fit the CKM matrices and quark masses under experimental uncertainties.

To understand the flavour parameters in RS model, we follow the approach of Ref. [9]. In our model we got 3×3 complex matrices of 5-D Yukawa couplings $Y_{u,d}^{(5)}$, each contains 9 real and 9 complex parameters. In RS model we get additional flavour parameters through 3×3 Hermitian bulk mass matrices, $c_{Q,u,d}$. This brings in additional 18 real parameters and 9 complex phases.

For Numerical scan it is convenient to work in the basis where the bulk mass matrices $c_{Q,u,d}$ are diagonal and comprise of 9 real parameters. The remaining 18 real parameters and 10 physical phases are then collected in the 5D Yukawa coupling matrices $Y_{u,d}^{(5)}$.

We use the parameterisation adopted in the [46], where the bulk mass matrices are real and diagonal. We derive the parameterisation of the unitary matrices $U_{l,r}$ and $D_{l,r}$ generalizing the usual CKM parameterisation, as product of three rotations and introducing a complex phases in each of them [47], this parameterisation ensures the information about only the physical parameters. We therefore aim to derive a parameterisation of the RS flavour sector in terms of the SM quark masses, the CKM parameters, and the parameters of the new flavour mixing matrices D_l , U_r and D_r . Neglecting the mixing with fermionic KK

modes and approximating the Higgs field to be exactly localised on the IR brane, we can write

$$\xi_u = U_l^\dagger Y_u U_r, \quad (42)$$

$$\xi_d = D_l^\dagger Y_d D_r \quad (43)$$

where $Y_{u,d}$ are effective 4D couplings defined in Eq.(10) and $\xi_{u,d}$ are defined as

$$\xi_u = \frac{\sqrt{2}}{v} \text{diag}(m_u, m_c, m_t), \quad \xi_d = \frac{\sqrt{2}}{v} \text{diag}(m_d, m_s, m_b) \quad (44)$$

The CKM matrix is given by

$$U_l^\dagger D_l = V_{\text{CKM}}. \quad (45)$$

The 5D Yukawa couplings can then be written as

$$\begin{aligned} \left(Y_u^{(5)}\right)_{ij} &= f^{(0)-1}(c_{Qi}) \left(U_l \xi_u U_r^\dagger\right)_{ij} f^{(0)-1}(c_{uj}) \\ &= f^{(0)-1}(c_{Qi}) \left(D_l V_{\text{CKM}}^\dagger \xi_u U_r^\dagger\right)_{ij} f^{(0)-1}(c_{uj}), \end{aligned} \quad (46)$$

$$\left(Y_d^{(5)}\right)_{ij} = f^{(0)-1}(c_{Qi}) \left(U_l \xi_d U_r^\dagger\right)_{ij} f^{(0)-1}(c_{dj}), \quad (47)$$

In the above parametrization, the SM parameters are encoded in the quark masses and V_{CKM} . 9 new real flavour parameters are present in $c_{Q,u,d}$. The remaining 9 real parameters and 9 complex phases are distributed among D_l , U_r and D_r .

We use CKM parameterisation, as a product of three rotations, and introducing a complex phase in each of them, thus obtaining product of three rotation matrices with angle $\omega_{ij}^{D_l}$ ($i, j = 1, 2, 3$) a complex phase $\tau_{ij}^{D_l}$ ($i, j = 1, 2, 3$) in each of them [48], Defining

$$c_{ij}^{D_l} = \cos \omega_{ij}^{D_l}, \quad s_{ij}^{D_l} = \sin \omega_{ij}^{D_l} \quad (i, j = 1, 2, 3). \quad (48)$$

parameterisation of D_l reads [48]

$$D_l = \begin{pmatrix} c_{12}^{D_l} c_{13}^{D_l} & s_{12}^{D_l} c_{13}^{D_l} e^{-i\tau_{12}^{D_l}} & s_{13}^{D_l} e^{-i\tau_{13}^{D_l}} \\ -s_{12}^{D_l} c_{23}^{D_l} e^{i\tau_{12}^{D_l}} - c_{12}^{D_l} s_{23}^{D_l} s_{13}^{D_l} e^{i(\tau_{13}^{D_l} - \tau_{23}^{D_l})} & c_{12}^{D_l} c_{23}^{D_l} - s_{12}^{D_l} s_{23}^{D_l} s_{13}^{D_l} e^{i(\tau_{13}^{D_l} - \tau_{12}^{D_l} - \tau_{23}^{D_l})} & s_{23}^{D_l} c_{13}^{D_l} e^{-i\tau_{23}^{D_l}} \\ s_{12}^{D_l} s_{23}^{D_l} e^{i(\tau_{12}^{D_l} + \tau_{23}^{D_l})} - c_{12}^{D_l} c_{23}^{D_l} s_{13}^{D_l} e^{i\tau_{13}^{D_l}} & -c_{12}^{D_l} s_{23}^{D_l} e^{i\tau_{23}^{D_l}} - s_{12}^{D_l} c_{23}^{D_l} s_{13}^{D_l} e^{i(\tau_{13}^{D_l} - \tau_{12}^{D_l})} & c_{23}^{D_l} c_{13}^{D_l} \end{pmatrix} \quad (49)$$

U_r and D_r are written in a completely analogous way. In order to naturally obtain anarchic 5D Yukawa matrices $\left(Y_{u,d}^{(5)}\right)$, it can in practice be useful to adapt the above parameterisation. The phases $\tau_{ij}^{D_l}$, $\tau_{ij}^{U_r}$ and $\tau_{ij}^{D_r}$ are all chosen to lie in their natural range $0 \leq \tau < 2\pi$, however the case of the mixing angles $\omega_{ij}^{D_l}$, $\omega_{ij}^{U_r}$ and $\omega_{ij}^{D_r}$ is somewhat different. Here one finds [9] that anarchic 5D Yukawa couplings imply the hierarchies

$$\omega_{ij}^{D_l} \sim \frac{f^{(0)}(c_{Qi})}{f^{(0)}(c_{Qj})}, \quad \omega_{ij}^{U_r} \sim \frac{f^{(0)}(c_{ui})}{f^{(0)}(c_{uj})}, \quad \omega_{ij}^{D_r} \sim \frac{f^{(0)}(c_{di})}{f^{(0)}(c_{dj})}. \quad (50)$$

We can now use this knowledge to find a parameterisation that automatically leads to a natural structure for $Y_{u,d}^{(5)}$. Therefore we define

$$\omega_{ij}^{D_l} = \epsilon_{ij}^{D_l} \frac{f^{(0)}(c_{Qi})}{f^{(0)}(c_{Qj})}, \quad \omega_{ij}^{U_r} = \epsilon_{ij}^{U_r} \frac{f^{(0)}(c_{ui})}{f^{(0)}(c_{uj})}, \quad \omega_{ij}^{D_r} = \epsilon_{ij}^{D_r} \frac{f^{(0)}(c_{di})}{f^{(0)}(c_{dj})}, \quad (51)$$

where $\epsilon_{ij}^{D_l}, \epsilon_{ij}^{U_r}, \epsilon_{ij}^{D_r}$ are $\mathcal{O}(1)$ parameters. We choose to scan over the following independent variables $c_{Q,u,d}$, $U_{l,r}$ and $D_{l,r}$, then we check whether the 5D Yukawa is anarchic and satisfy the condition $0.1 \leq |Y_{u,d_{ij}}^{(5)}| \leq 3$. The rough choice of c values of fermions for anarchic 5-D Yukawa couplings are approximated using rough

Parameter	Value \pm Error
m_t	$(136.2 \pm 3.1) \text{ GeV}$
m_b	$(2.4 \pm 0.04) \text{ GeV}$
m_c	$(0.56 \pm 0.04) \text{ GeV}$
m_s	$(0.047 \pm 0.012) \text{ MeV}$
m_d	$(2.0 \pm 4.0) \text{ MeV}$
m_u	$(1.2 \pm 0.4) \text{ MeV}$

Table 4: Quark \overline{MS} masses at 3 TeV [25].

size of the mixing angles given by [49]:

$$|D_l|_{ij} \sim \frac{f^{(0)}(c_{Qi})}{f^{(0)}(c_{Qj})}, \quad |D_r|_{ij} \sim \frac{f^{(0)}(c_{di})}{f^{(0)}(c_{dj})}, \quad |U_r|_{ij} \sim \frac{f^{(0)}(c_{ui})}{f^{(0)}(c_{uj})}, \quad i \leq j \quad (52)$$

We can also get that $|V_{CKM}|_{ij} \sim \frac{f^{(0)}(c_{Qi})}{f^{(0)}(c_{Qj})}$, thus the hierarchy in CKM elements is purely set by the c_Q . The hierarchy in the mass eigenvalues are given as:

$$(m_{u,d})_i \sim \frac{v}{\sqrt{2}} Y f^{(0)}(c_{Qi}) f^{(0)}(c_{u,di}) \quad (53)$$

The CKM and the mass eigenvalues fixes the $f^{(0)}(c_{Q,u,d})$ in terms of CKM parameters and fermions masses as (assuming $f^{(0)}(c_{u3}) \sim \mathcal{O}(1)$):

$$f^{(0)}(c_{Q2})/f^{(0)}(c_{Q3}) \sim \lambda^2, \quad f^{(0)}(c_{Q1})/f^{(0)}(c_{Q3}) \sim \lambda^3, \quad f^{(0)}(c_{d3}) \sim \frac{m_b}{m_t}, \quad f^{(0)}(c_{u2}) \sim \frac{m_c}{m_t} \frac{1}{\lambda^2},$$

$$f^{(0)}(c_{d2}) \sim \frac{m_s}{m_t} \frac{1}{\lambda^2}, \quad f^{(0)}(c_{u1}) \sim \frac{m_u}{m_t} \frac{1}{\lambda^3}, \quad f^{(0)}(c_{d1}) \sim \frac{m_d}{m_t} \frac{1}{\lambda^3}, \quad (54)$$

where $\lambda \sim 0.22$. For simplicity of numerical analysis, we randomly vary each set of the independent c values around their natural size Eq.(54) by a factor of three. The diagonalization matrix is calculated using the above mentioned technique. The masses of quarks used in this work is given in Table 4. We choose the c_{Q3} from Ref.[26, 21] which allows for consistency with electro-weak precision data as to satisfy the $Z \rightarrow b_l \bar{b}_l$.

References

- [1] G. Buchalla, A. J. Buras, and M. E. Lautenbacher, “Weak decays beyond leading logarithms,” *Rev. Mod. Phys.*, vol. 68, pp. 1125–1144, 1996.
- [2] A. J. Buras, “Weak Hamiltonian, CP violation and rare decays,” in *Les Houches Summer School in Theoretical Physics, Session 68: Probing the Standard Model of Particle Interactions*, pp. 281–539, 6 1998.

- [3] G. Isidori, Y. Nir, and G. Perez, “Flavor Physics Constraints for Physics Beyond the Standard Model,” *Ann. Rev. Nucl. Part. Sci.*, vol. 60, p. 355, 2010.
- [4] S. Gori, “Three Lectures of Flavor and CP violation within and Beyond the Standard Model,” in *2015 European School of High-Energy Physics*, pp. 65–90, 2017.
- [5] J. Zupan, “Introduction to flavour physics,” *CERN Yellow Rep. School Proc.*, vol. 6, pp. 181–212, 2019.
- [6] L. Randall and R. Sundrum, “An alternative to compactification,” *Physical Review Letters*, vol. 83, p. 4690–4693, Dec 1999.
- [7] L. Randall and R. Sundrum, “Large mass hierarchy from a small extra dimension,” *Physical Review Letters*, vol. 83, p. 3370–3373, Oct 1999.
- [8] K. Agashe, A. Delgado, M. J. May, and R. Sundrum, “RS1, custodial isospin and precision tests,” *JHEP*, vol. 08, p. 050, 2003.
- [9] K. Agashe, G. Perez, and A. Soni, “Flavor structure of warped extra dimension models,” *Phys. Rev.*, vol. D71, p. 016002, 2005.
- [10] H. Davoudiasl, G. Perez, and A. Soni, “The Little Randall-Sundrum Model at the Large Hadron Collider,” *Phys. Lett.*, vol. B665, pp. 67–71, 2008.
- [11] H. Davoudiasl, S. Gopalakrishna, and A. Soni, “Big signals of little randall–sundrum models,” *Physics Letters B*, vol. 686, p. 239–243, Mar 2010.
- [12] M. Bauer, S. Casagrande, L. Grunder, U. Haisch, and M. Neubert, “Little Randall-Sundrum models: epsilon(K) strikes again,” *Phys. Rev. D*, vol. 79, p. 076001, 2009.
- [13] G. Dvali, G. Gabadadze, and M. Porrati, “4-D gravity on a brane in 5-D Minkowski space,” *Phys. Lett. B*, vol. 485, pp. 208–214, 2000.
- [14] H. Georgi, A. K. Grant, and G. Hailu, “Brane couplings from bulk loops,” *Phys. Lett. B*, vol. 506, pp. 207–214, 2001.
- [15] M. Carena, E. Ponton, T. M. P. Tait, and C. E. M. Wagner, “Opaque branes in warped backgrounds,” *Phys. Rev.*, vol. D67, p. 096006, 2003.
- [16] M. Carena, A. Delgado, E. Ponton, T. M. Tait, and C. Wagner, “Precision electroweak data and unification of couplings in warped extra dimensions,” *Phys. Rev. D*, vol. 68, p. 035010, 2003.
- [17] J. Santiago, “Minimal Flavor Protection: A New Flavor Paradigm in Warped Models,” *JHEP*, vol. 12, p. 046, 2008.
- [18] T. Gherghetta and A. Pomarol, “Bulk fields and supersymmetry in a slice of AdS,” *Nucl. Phys. B*, vol. 586, pp. 141–162, 2000.

- [19] C. Csaki, J. Erlich, and J. Terning, “The Effective Lagrangian in the Randall-Sundrum model and electroweak physics,” *Phys. Rev. D*, vol. 66, p. 064021, 2002.
- [20] M. E. Peskin and T. Takeuchi, “Estimation of oblique electroweak corrections,” *Phys. Rev.*, vol. D46, pp. 381–409, 1992.
- [21] S. Casagrande, F. Goertz, U. Haisch, M. Neubert, and T. Pfoh, “Flavor Physics in the Randall-Sundrum Model: I. Theoretical Setup and Electroweak Precision Tests,” *JHEP*, vol. 10, p. 094, 2008.
- [22] A. M. Iyer, K. Sridhar, and S. K. Vempati, “Bulk Randall-Sundrum models, electroweak precision tests, and the 125 GeV Higgs,” *Phys. Rev. D*, vol. 93, no. 7, p. 075008, 2016.
- [23] M. Aaboud, G. Aad, B. Abbott, O. Abdinov, B. Abeloos, S. H. Abidi, O. S. AbouZeid, N. L. Abraham, H. Abramowicz, and et al., “Search for heavy particles decaying into top-quark pairs using lepton-plus-jets events in proton–proton collisions at $\sqrt{s} = 13\text{TeV}$ with the atlas detector,” *The European Physical Journal C*, vol. 78, Jul 2018.
- [24] A. Belyaev, N. D. Christensen, and A. Pukhov, “CalcHEP 3.4 for collider physics within and beyond the Standard Model,” *Comput. Phys. Commun.*, vol. 184, pp. 1729–1769, 2013.
- [25] C. Csaki, A. Falkowski, and A. Weiler, “The Flavor of the Composite Pseudo-Goldstone Higgs,” *JHEP*, vol. 09, p. 008, 2008.
- [26] M. Bauer, S. Casagrande, U. Haisch, and M. Neubert, “Flavor Physics in the Randall-Sundrum Model: II. Tree-Level Weak-Interaction Processes,” *JHEP*, vol. 09, p. 017, 2010.
- [27] K. Agashe, A. Azatov, and L. Zhu, “Flavor Violation Tests of Warped/Composite SM in the Two-Site Approach,” *Phys. Rev. D*, vol. 79, p. 056006, 2009.
- [28] M. Blanke, A. J. Buras, B. Duling, S. Gori, and A. Weiler, “ $\Delta F=2$ Observables and Fine-Tuning in a Warped Extra Dimension with Custodial Protection,” *JHEP*, vol. 03, p. 001, 2009.
- [29] A. Ahmed, A. Carmona, J. Castellano Ruiz, Y. Chung, and M. Neubert, “Dynamical origin of fermion bulk masses in a warped extra dimension,” *JHEP*, vol. 08, p. 045, 2019.
- [30] M. Ciuchini *et al.*, “Delta M(K) and epsilon(K) in SUSY at the next-to-leading order,” *JHEP*, vol. 10, p. 008, 1998.
- [31] M. Ciuchini, E. Franco, V. Lubicz, G. Martinelli, I. Scimemi, and L. Silvestrini, “Next-to-leading order QCD corrections to Delta F = 2 effective Hamiltonians,” *Nucl. Phys.*, vol. B523, pp. 501–525, 1998.
- [32] M. Bona *et al.*, “Model-independent constraints on $\Delta F = 2$ operators and the scale of new physics,” *JHEP*, vol. 03, p. 049, 2008.
- [33] J. A. Bagger, K. T. Matchev, and R.-J. Zhang, “Qcd corrections to flavor-changing neutral currents in the supersymmetric standard model,” *Physics Letters B*, vol. 412, p. 77–85, Oct 1997.

- [34] A. J. Buras, M. Misiak, and J. Urban, “Two-loop qcd anomalous dimensions of flavour-changing four-quark operators within and beyond the standard model,” *Nuclear Physics B*, vol. 586, p. 397–426, Oct 2000.
- [35] R. Barbieri, G. Isidori, J. Jones-Perez, P. Lodone, and D. M. Straub, “ $U(2)$ and Minimal Flavour Violation in Supersymmetry,” *Eur. Phys. J. C*, vol. 71, p. 1725, 2011.
- [36] R. Barbieri, G. Isidori, A. Pattori, and F. Senia, “Anomalies in B -decays and $U(2)$ flavour symmetry,” *Eur. Phys. J. C*, vol. 76, no. 2, p. 67, 2016.
- [37] G. D’Ambrosio, G. Giudice, G. Isidori, and A. Strumia, “Minimal flavor violation: An Effective field theory approach,” *Nucl. Phys. B*, vol. 645, pp. 155–187, 2002.
- [38] A. Fitzpatrick, G. Perez, and L. Randall, “Flavor anarchy in a Randall-Sundrum model with 5D minimal flavor violation and a low Kaluza-Klein scale,” *Phys. Rev. Lett.*, vol. 100, p. 171604, 2008.
- [39] G. Isidori, “Model building on flavour anomalies and implications for high-pt searches at implications of lhcb measurements and future prospects, cern geneva,” Nov 2017.
- [40] M. Bordone, O. Cata, T. Feldmann, and R. Mandal, “Constraining flavour patterns of scalar leptoquarks in the effective field theory,” 10 2020.
- [41] W. Altmannshofer, S. Gori, M. Pospelov, and I. Yavin, “Quark flavor transitions in $L_\mu - L_\tau$ models,” *Phys. Rev. D*, vol. 89, p. 095033, 2014.
- [42] A. Crivellin, G. D’Ambrosio, and J. Heeck, “Addressing the LHC flavor anomalies with horizontal gauge symmetries,” *Phys. Rev. D*, vol. 91, no. 7, p. 075006, 2015.
- [43] A. Crivellin, “B-anomalies related to leptons and lepton flavour universality violation,” *PoS*, vol. BEAUTY2016, p. 042, 2016.
- [44] D. Buttazzo, A. Greljo, G. Isidori, and D. Marzocca, “B-physics anomalies: a guide to combined explanations,” *JHEP*, vol. 11, p. 044, 2017.
- [45] G. Hiller, “Flavor theory 2020 and outlook having fun with leptons: B-anomalies and more, ichep2020 prague,”
- [46] M. E. Albrecht, M. Blanke, A. J. Buras, B. Duling, and K. Gemmler, “Electroweak and Flavour Structure of a Warped Extra Dimension with Custodial Protection,” *JHEP*, vol. 09, p. 064, 2009.
- [47] J. A. Casas and A. Ibarra, “Oscillating neutrinos and muon $\rightarrow e, \gamma$,” *Nucl. Phys.*, vol. B618, pp. 171–204, 2001.
- [48] M. Blanke, A. J. Buras, A. Poschenrieder, S. Recksiegel, C. Tarantino, S. Uhlig, and A. Weiler, “Another look at the flavour structure of the littlest Higgs model with T-parity,” *Phys. Lett.*, vol. B646, pp. 253–257, 2007.
- [49] S. J. Huber, “Flavor violation and warped geometry,” *Nucl. Phys.*, vol. B666, pp. 269–288, 2003.